The effects of sintering temperature and current contacting layer on the performance of lanthanum nickelate electrodes in Solid Oxide Fuel Cells

Harrison, Chris; Sarruf, Bernardo; Klotz, D; Slater, Peter; Steinberger-Wilckens, Robert

DOI:
10.1016/j.ssi.2023.116386

Document Version
Publisher's PDF, also known as Version of record

Citation for published version (Harvard):
Harrison, C, Sarruf, B, Klotz, D, Slater, P & Steinberger-Wilckens, R 2023, 'The effects of sintering temperature and current contacting layer on the performance of lanthanum nickelate electrodes in Solid Oxide Fuel Cells', *Solid State Ionics*. https://doi.org/10.1016/j.ssi.2023.116386

Solid State Ionics 403 (2023) 116386

Contents lists available at ScienceDirect

Solid State Ionics

journal homepage: www.elsevier.com/locate/ssi

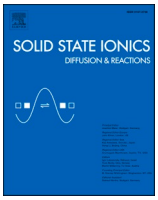

The effects of sintering temperature and current contacting layer on the performance of lanthanum nickelate electrodes in Solid Oxide Fuel Cells

C.M. Harrison [a,*], B.J.M. Sarruf [a], D. Klotz [c], P.R. Slater [b], R. Steinberger-Wilckens [a]

[a] School of Chemical Engineering, University of Birmingham, UK
[b] School of Chemistry, University of Birmingham, UK
[c] International Institute for Carbon-Neutral Energy Research (I^2CNER), Kyushu University, Japan

ARTICLE INFO

Keywords:
Solid oxide fuel cell
SOFC
Cathode
$La_2NiO_{4+\delta}$
Sintering temperature

ABSTRACT

The Ruddlesden-Popper phase $La_2NiO_{4+\delta}$ (LNO214) has received a significant level of research attention with respect to its employment as a Solid Oxide Fuel Cell cathode material. However, it is known that there are many factors that are capable of influencing the performance of this phase when utilised in this role. One such factor that can impact on electrode behaviour is the choice of sintering temperature. In this paper, a study of this effect is detailed. This is achieved via the use of both symmetrical and single cell testing configurations, with additional investigation provided by ex-situ analysis. It is shown that a sizeable improvement in electrode performance can be achieved via an increase in sintering temperature. This is despite observations on the reactivity between LNO214 and the contact electrolyte material $Ce_{0.9}Gd_{0.1}O_{2-\delta}$. Further, it is also demonstrated that the addition of a noble metal contacting layer can dramatically improve the performance of an LNO214 electrode. In comparison, the impact of a contacting layer on a state-of-the-art $La_{0.6}Sr_{0.4}Co_{0.2}Fe_{0.8}O_{3-\delta}$ composition is shown to be relatively minor. This has implications towards SOFC testing methodologies given the widespread employment of noble metal contacting pastes.

1. Introduction

The research and development of solid oxide fuel cell (SOFC) materials over the last few decades has driven a dramatic improvement in cell performance and lifetime [1,2]. Significantly, and in the wake of a global energy transition, these advancements have helped to bring about a commercialisation of this low-carbon technology. There remains a sense within the academic literature, however, that further improvements can be offered with respect to the long-term stability of SOFC components. Perhaps most notably, researchers have sought to engineer resilient, high-performing oxygen electrode materials [3]. Such materials are intended to provide an alternative to the state-of-the-art lanthanum cobaltite-type perovskites (LSCF and LSC) that are widely employed in the commercial cells of today. This focus of exploring new metal oxide materials is with a view to overcoming perceived problems relating to the use of Sr and Co in those aforementioned state-of-the-art materials. In the first case, authors have observed the issue of SrO segregation and corresponding degradation phenomena which result in a loss of power output over time [4–6]. The most significant drawback relates to 'chromium poisoning'. Here, SrO reacts with chromium hydroxide to form insulating and deactivating phases (e.g. $SrCrO_4$) [3], leading to dramatic loss of cell output over time. Further to these performance related problems, concerns have also been raised relating to a reliance on cobalt-containing materials in the development of future energy technologies [7]. Not only does such a reliance offer ethical, environmental and financial concerns but, in the specific case of SOFC, this also introduces some challenges relating to differential thermal expansion coefficients with respect to common electrolyte materials (e.g. ZrO_2- and CeO_2- based materials) [8].

One body of materials that has received substantial attention in the area of SOFC materials development is the lanthanum nickelates [9,10]. This includes perovskite-type (doped-$LaNiO_3$) phases in addition to the structurally-related Ruddlesden-Popper-type ($La_{n+1}Ni_nO_{3n+1}$) phases. Analysis of the literature shows that these materials demonstrate a very broad range of properties (from materials with excellent electronic conductivity, to materials with excellent oxygen transport properties) [9,11]. The first-order ($n = 1$) Ruddlesden-Popper phase $La_2NiO_{4+\delta}$ has received particular interest for employment as an oxygen electrode material [12–14]. In addition to excellent oxygen transport behaviour, the lanthanum nickelates are perceived to offer improved resilience to

* Corresponding author.
E-mail address: c.harrison.1@bham.ac.uk (C.M. Harrison).

https://doi.org/10.1016/j.ssi.2023.116386
Received 22 July 2023; Received in revised form 25 September 2023; Accepted 16 October 2023
Available online 24 October 2023

chromium poisoning [3]. However, considerations of the data within the literature indicate that the achievable performance is inferior to that of LSCF electrodes. This can be seen in terms of polarisation resistance (R_{pol}) values from symmetrical cell testing [12,15–31] and in terms of current output measured in single cell tests [2,26,32–37]. A further analysis of this data, alongside that recorded in the study presented here, is considered later in this article. However, comparisons between studies are subject to a number of caveats. Firstly, a great variation in the performance metrics of $La_2NiO_{4+\delta}$ is seen from study to study. This is likely a result of differences in details of cell materials, fabrication conditions, and testing configurations. The role of sintering temperature is one such potential difference. There is evidence in the literature to suggest that lower sintering temperatures may be favourable for lanthanum nickelate materials when paired with CeO_2-based electrolytes due to chemical incompatibility issues [38,39]. However, whilst there is often discussion on the reaction between these materials, this does not account for the performance of electrodes sintered under different conditions (i.e. whether or not higher sintering temperatures actually offer a detrimental impact). Results from recent studies [40,41] indicate that higher sintering temperatures can actually improve the observed performance of $La_2NiO_{4+\delta}$ electrodes, although we note that this finding appears to contradict an earlier article in this area [30]. A difficulty that can be noted when surveying the literature is in drawing comparisons with LSCF electrodes. Different materials (e.g. electrolytes and contact materials) and testing approaches make it challenging to obtain an understanding of the relative suitability of lanthanum nickelates in comparison with commercial state-of-the-art materials. From an analysis of the literature data, it would appear that $La_2NiO_{4+\delta}$ offers relatively poor performance in comparison with LSCF. However, a major caveat is that comparisons between data often require consideration across numerous studies and thus such analysis may not necessarily be fair. In this study, an assessment of the effects of sintering temperature on the performance of $La_2NiO_{4+\delta}$ is described. Further, direct comparisons with conventional electrodes (commercial $La_{0.6}Sr_{0.4}Co_{0.2}Fe_{0.8}O_3$ – i.e. LSCF6428) are shown in order to offer context. The analysis detailed here covers both in-situ and ex-situ techniques to offer a more comprehensive understanding of the achievable performance of $La_2NiO_{4+\delta}$ and the factors that contribute to differences in performance.

2. Experimental

2.1. Sample preparation

For this study, the Pechini route was employed to synthesise the $La_2NiO_{4+\delta}$ phase. This process has also been utilised elsewhere in the literature and enables the material in question to be prepared quickly and with relative ease [42,43]. Briefly, stoichiometric quantities of lanthanum (III) nitrate hexahydrate and nickel (II) nitrate hexahydrate were dissolved in deionised water. With the solution continually stirred on a hot plate ($T = 80$ °C), citric acid and ethylene glycol were then added to enable the formation of a polymeric gel (see [44]). The resulting gel was heated to 350 °C to form an ash-like pre-cursor, prior to a final annealing step at 1100 °C to synthesise the desired phase. To ensure the anticipated phase had been achieved, phase analysis was performed via X-Ray Diffraction (XRD), using a D2 Bruker Diffractometer (Co-$K_\alpha = 0.179$ nm, 10 mA current, and 30 kV accelerating voltage). The ICSD and PDF databases were used for the identification of phases. The successfully synthesised materials were ball-milled and then sieved (25 μm mesh) to remove any larger agglomerates. To form electrodes, an ink was prepared by combining the $La_2NiO_{4+\delta}$ powder with a commercial Terpineol-based ink vehicle (FuelCellMaterials). The resulting slurry was then homogenised using a triple roll mill and brush-painted[1] onto commercial 5 × 5 cm^2 electrolyte substrates acquired from SOFCMan. In the case of symmetrical cell testing, this substrate was an 8 mol% yttria-stabilised zirconia (8YSZ) electrolyte support (200 μm) with 10 mol% gadolinia-doped ceria (GDC-10) layers (5 μm) applied to both sides. For single cell testing, anode-supported half-cell substrates were procured. These comprised of a Ni-8YSZ anode (400 μm), 8YSZ electrolyte (10–15 μm) and GDC-10 barrier layer (2–3 μm). The wet electrode layers were dried and then sintered at several different temperatures (1000 to 1150 °C) for 4 h. For reference, lanthanum strontium cobalt ferrite (LSCF6428) electrodes were also tested using a commercial powder acquired from Praxair ($La_{0.6}Sr_{0.4}Co_{0.2}Fe_{0.8}O_3$; 99.9% purity).

2.2. Symmetrical cell testing

The symmetrical cells (prepared in accordance with 2.1) were tested in static air, using a 4-point connection set-up. Each test was conducted in an identical fashion with the same apparatus. In the first batch of tests, current collection was provided by two 16 cm^2 Au contact meshes (Fiaxell, Switzerland). These were placed in direct contact with the two sintered electrodes. A 175 g alumina weight was placed on top of the assembly to hold the mesh in place and improve the contact between the mesh and the electrode. The resulting assembly was then heated up to 600 °C in a Carbolite furnace and held at temperature for 12 h. Electrochemical Impedance Spectroscopy (EIS) measurements were recorded using a Solatron Potentiostat (1470E and 1455FRA). Measurements were taken using a perturbation amplitude of 10 mV (2 cycles integration, 1 cycle delay). EIS measurements were performed up to 800 °C in intervals of 50 °C (for each measurement, the furnace was held at the given temperature for 1 h to allow the cell to reach a steady state). The cell was then held for a further 12 h prior to the commencement of the cool-down cycle when measurements were taken in an identical fashion. For the tests considering the impact of the gold contacting layer, the samples were re-tested after the application of a commercial Au-ink (Fuel Cell Materials). In this instance, a layer of gold ink (70 mass% gold) was brush-painted on top of the electrodes and dried at 100 °C.

2.3. Single cell testing

For single cell testing purposes, a commercial SOFC test station (Chino Corporation) was employed. Current collection was achieved using Ag- and Ni-foam meshes on the cathode and anode sides of the cell, respectively. For improved electrical contact on the cathode side of the cell, Au-paste (*Fuel Cell Materials)* was applied and dried at 100 °C. Sealing was achieved using mica gasket frames. Humidified hydrogen and dry air were supplied to the cell via Bronkhorst mass flow controllers with the ability to dilute both fuel and oxidant streams with nitrogen. Electrochemical measurements were performed with a Solatron Potentiostat (1470E and 1455FRA) in series with a Solatron booster system. For voltage-current curves, a potential-step programme was applied, stepping the voltage in 10 mV intervals and measuring the current for 30 s. A similar approach to voltage-current measurements

[1] In an attempt to control layer thickness, the applied ink mass was kept consistent in each case. Post-test SEM analysis suggested a layer thickness of between 10 and 30 μm was obtained via this route (see Supplementary Figure S4 and Figure S5 for examples). We anticipate this range could have some role on electrochemical performance but we find the results and relationships observed in this paper to be consistent across the results of both symmetrical and single cell testing.

was recommended in [45]. EIS was performed with a 50 mV perturbation signal[2] (2 cycles integration, 1 cycle delay) at frequencies between 10 MHz and 0.05 Hz.

2.4. Data analysis

The impedance data for each test were analysed using ZView. The ohmic (R_o) resistance was determined from the high frequency intercept, whereas the polarisation resistance (R_{pol}) was determined by the difference between the high and low frequency (Z'_{LF}) intercepts. In all cases, the data was normalised by the area of the electrode (S). In the case of the symmetrical cell tests, and as is common convention in the literature,[3] the R_{pol} value was divided by two to account for the number of electrodes. In this case:

$$R_{pol} = Z'_{LF} - R_o \left(\frac{S}{2}\right).$$

For single cell testing, a Distribution of Relaxation Times (DRT) analysis was employed using an in-house developed MATLAB code. This approach contributed towards the Equivalent Circuit Modelling (ECM) of the impedance data and helped identify the number of processes contributing to the response (as well as offering insight into their magnitude and characteristic frequency). Using these data to provide starting values, a Complex Non-Linear Least Squares (CNLS) fitting technique was employed (*ZView)* to provide an assessment of the polarisation and ohmic contributions associated with each electrode.

2.5. Ex-situ analysis

To complement the in-situ analysis of electrode performance, further experiments were conducted to offer additional insight into the effects of sintering temperature on the $La_2NiO_{4+\delta}$ electrodes. High magnification imaging was conducted on the samples, using a Scanning Electron Microscope (Phillips XL30 ESEM FEG). To prepare samples for imaging, cells were first mounted in epoxy resin (Buehler). These samples were then ground and polished to expose the cross-section of the cell. Finally, the polished samples were sputter-coated prior to imaging. Further to post-test analysis, a series of experiments were conducted using a DIL-404C Netzsch dilatometer to understand the relative sintering behaviour of $La_2NiO_{4+\delta}$ compared with more conventional SOFC electrode materials. In this instance, green (un-sintered) pellets of several materials were prepared using a pellet press. The green pellets were then carefully loaded into the dilatometer. The pellets were heated to a selected sintering temperature at a heating rate of 5 °C/min and held for 4 h. These tests were conducted to assess the sintering behaviour of the green bodies (and hence the phases) under different temperatures.

3. Results and discussion

3.1. Synthesis

Synthesis of $La_2NiO_{4+\delta}$ via the aforementioned Pechini route was found to offer a facile means by which the desired phase could be prepared. The XRD data taken from a scan of the final sample (after ball-milling and sieving) are shown in Fig. 1. The data compared favourably with that taken from the ICSD database (database number #44121 [46]). No peaks pertaining to any impurity phases were noted.

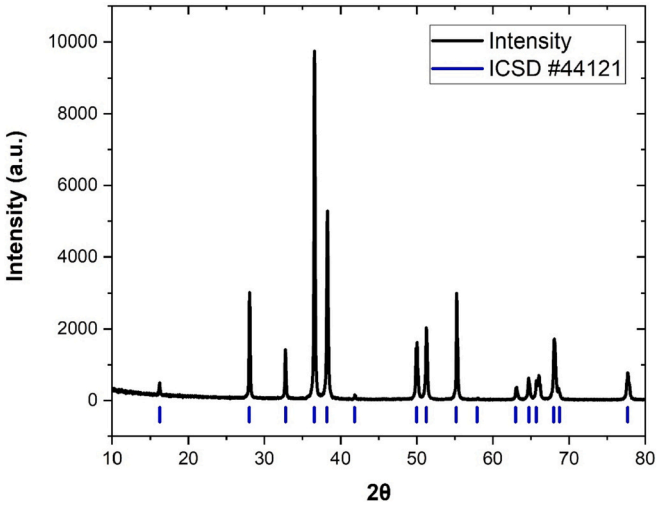

Fig. 1. XRD data taken from a sample of $La_2NiO_{4+\delta}$ prepared for this study, compared to database peak positions (ICSD). A version of this figure has been published in a PhD thesis [47].

3.2. Symmetrical cell testing

Results from symmetrical cell testing of $La_2NiO_{4+\delta}$ electrodes sintered at different temperatures are summarised in Fig. 2. The complete set of data, as represented in Nyquist form, are provided in the supplementary documentation (Fig. S1). In all instances the impedance spectra are normalised by the electrode area, and for comparative purposes, the ohmic contribution has been removed from the Nyquist plots but can be noted in Fig. 2c and Fig. 2d. As is observable from these data, there was a significant improvement in performance with increasing sintering temperature (i.e. a reduction in the impedance metrics). This is most keenly noted in its effect on the ohmic resistance (R_o). A reduction of R_o from 298 Ωcm^2 to 77.5 Ωcm^2 ($T_{Op} = 800$ °C) was found via an increase of the sintering temperature from 1000 to 1150 °C. This observation is explored in more detail, later. At higher sintering temperatures there was a considerable reduction in the measured polarisation resistance (R_{pol}) as shown in Fig. 2b to d. It was seen that R_{pol} could be reduced from 5.35 Ωcm^2 to 0.97 Ωcm^2 ($T_{Op} = 800$ °C) via an increase in sintering temperature. Other researchers have indicated that the electronic conductivity of $La_2NiO_{4+\delta}$ offers difficulties with respect to developing an electrode with suitable performance [48,49]. The evidence here suggests that this issue can be alleviated to some extent via a higher sintering temperature. Notably, this is despite some observations in the literature relating to reactions between $La_2NiO_{4+\delta}$ and CeO_2-phases (this is considered in more detail later in this paper). Interestingly, it is of note that additional experiments conducted on LSCF6428 electrodes sintered at various temperatures (see supplementary Fig. S2) did not show the same findings as observed with $La_2NiO_{4+\delta}$. In that case, the increased sintering temperatures led to inferior performance when employing commercial LSCF6428 material. This offers some insight into the different sintering behaviours of these two materials. The effects of sintering temperature will be studied in more detail later in this article.

To probe the effect of improving the contact resistance between the Au-mesh and the underlying electrode (which is one factor comprising the R_o), an additional set of tests was performed on the electrodes sintered at 1000 °C and 1150 °C. In these cases, an Au-contact paste (Fuel Cell Materials) was applied to the electrodes to act as a current collection layer (CCL) in addition to the Au-mesh. This sample was then tested once more under the same conditions, so as-to offer insight into the effect of improving current collection. The results from the tests conducted on the LNO214 electrodes sintered at 1000 °C are shown in Fig. 3a and b. The results of the tests conducted on the electrodes sintered at 1150 °C can be viewed in the supplementary material (see Fig. S3). The two sets of

[2] Although lower perturbation amplitudes are often used in the literature (e.g. 10–25 mV), the 50 mV perturbation amplitude was found to be necessary here, during preliminary testing – the authors believe that this perturbation remains within a pseudo-linear regime (as evidenced in Supplementary Figure S10). Kramers-Kronig results for these tests are also reported in Supplementary Figure S11.

[3] It is noted that there are some varying approaches to the calculation of R_{pol} in the literature. Generally, we find this to be the most common methodology that is applied.

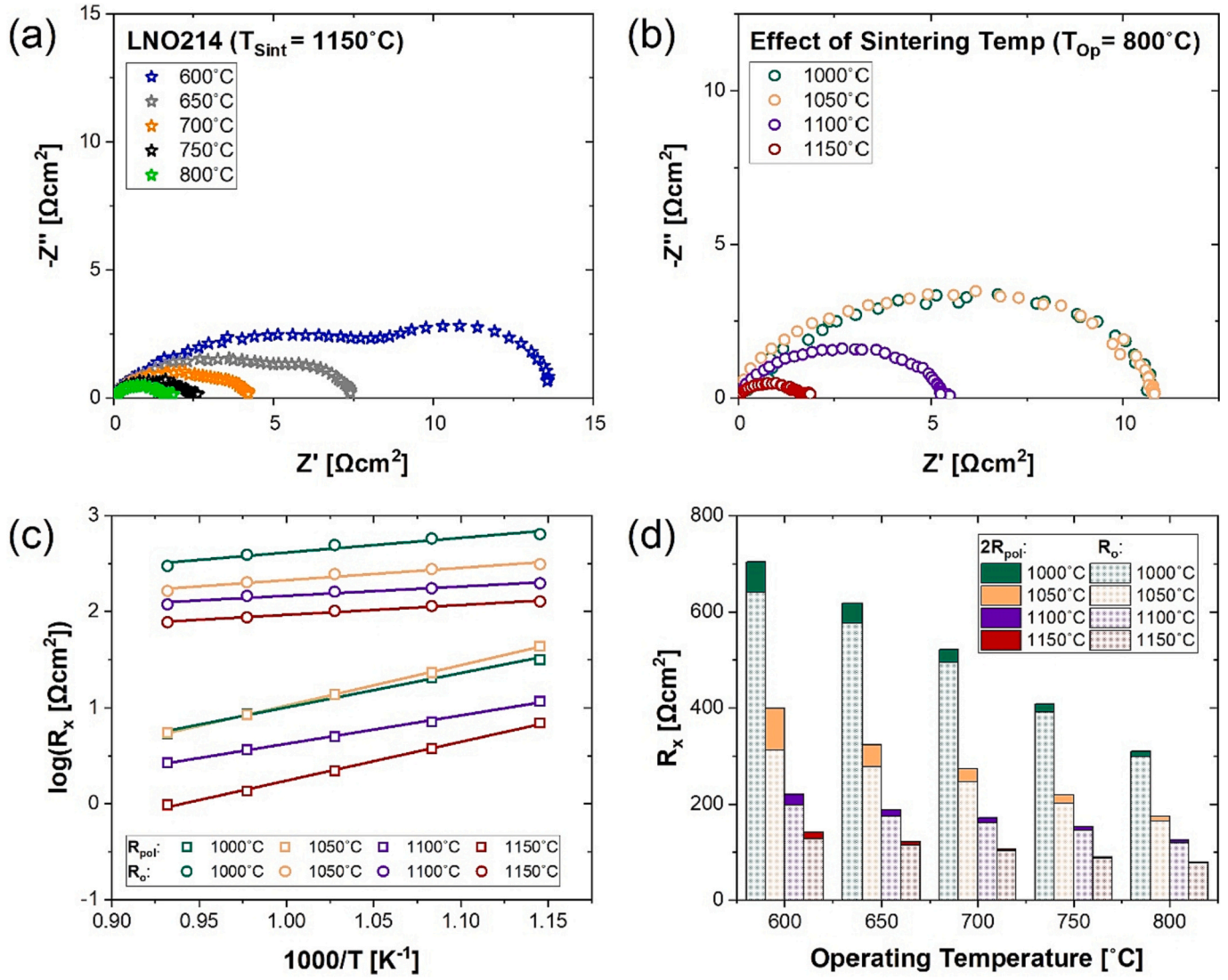

Fig. 2. EIS results from symmetrical cell tests; (a) normalised EIS results from $La_2NiO_{4+\delta}$ electrode sintered at 1150 °C, (b) effect of sintering temperature on EIS measurements at an operating temperature of 800 °C, (c) Arrhenius plots showing effect of temperature, (d) ohmic and polarisation resistance at various sintering and operating temperatures. Note: For Nyquist plots in this article, the impedance is normalised to the area of the electrode and the ohmic contribution has been removed; these plots therefore represent the polarisation resistance of both electrodes. For the final panel, two polarisation values (i.e. $2R_{pol}$) are shown alongside R_o to show the total Area Specific Resistance of the symmetrical cell. A version of this figure has been published in a PhD thesis [47].

tests (i.e. electrodes sintered at 1000 and 1150 °C) are compared in Fig. 4a and b. To offer further context, an identical approach was taken with electrodes fabricated from a commercial $La_{0.6}Sr_{0.4}Co_{0.2}Fe_{0.8}O_3$ powder (T_{Sint} = 1000 °C, 1150 °C). For the electrode sintered at 1000 °C the results are shown in Fig. 3c and d and, for the electrode sintered at 1150 °C, in the supplementary materials (Fig. S3). Arrhenius plots comparing the ohmic and polarisation resistances of the electrodes sintered at 1000 °C are shown in Fig. 3e and f, respectively. Several observations are evident. Firstly, the performance of the LSCF6428 electrode is generally seen to be superior to that of the $La_2NiO_{4+\delta}$ electrode. However, in the case of the latter material, a substantial improvement in electrode performance was achieved via the addition of the Au-CCL, particularly for the electrode sintered at 1000 °C (see Fig. 4). It can be noted that in this case there was an improvement in the data quality (i.e. reduced noise in the EIS spectra), and there was also a major reduction in R_o (from 298 Ωcm^2 at 800 °C to 0.96 Ωcm^2) and R_{pol} values (from 5.35 Ωcm^2 to 0.335 Ωcm^2) in the Arrhenius plots. In comparison, the addition of the Au-CCL to the LSCF6428 electrode had a less profound effect. Whilst the ohmic performance was certainly improved (i.e. 7.19 Ωcm^2 to 0.64 Ωcm^2 at 800 °C), and was similar to that measured from the $La_2NiO_{4+\delta}$-Au-CLL combination, the effect on polarisation resistance was much less evident. In fact, in the lower temperature range at least, the R_{pol} values increased. This performance loss was possibly a result of some degradation occurring between the experiments but, at least suggests the improved CCL does not hugely influence the polarisation performance of LSCF6428 in these tests. It is further notable from Fig. 4 that the impact of the Au-CCL layer on the R_{pol} values of the LSCF electrodes was marginal in both cases studied (T_{Sint} = 1000 °C, 1150 °C). In the case of LNO214, Fig. 4 shows that whilst the improvement in R_{pol} was generally more significant than the LSCF6428 case, the improvement was most profound for the electrode sintered at the lower temperature (which demonstrated the lower R_o values prior to the application of the Au-CCL). Perhaps more interestingly it is shown that the R_{pol} values of those tests are almost identical.

The activation energies (E_a) associated with both the R_{pol} and R_o measurements are shown in Table 1. Firstly, considering the E_a values associated with the R_o contribution, it can be seen that the application of the Au-paste led to much increased activation energy values in the case of both LSCF and LNO214. This observation (when also combined with observations on the R_o values themselves) appears to indicate that in,

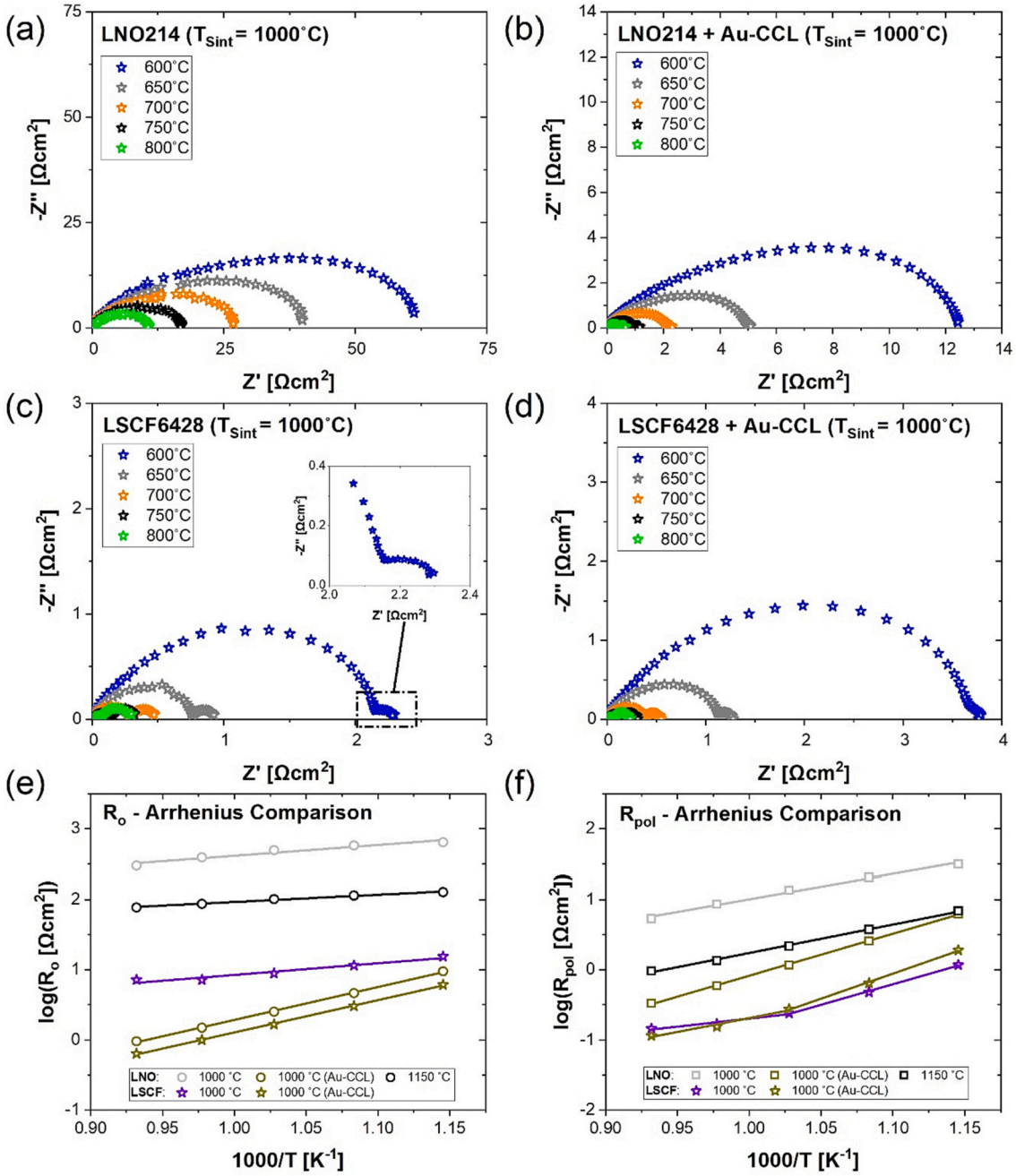

Fig. 3. The symmetrical cell impedance spectra of a $La_2NiO_{4+\delta}$ electrode sintered at 1000 °C in the (a) absence of an Au-Current Collector Layer (Au-CCL) and (b) with the subsequent addition of an Au-CCL. Comparative results taken for a commercial $La_{0.6}Sr_{0.4}Co_{0.2}Fe_{0.8}O_3$ electrode (c) without an Au-CCL and (d) with the addition of an Au-CCL. Arrhenius plots showing the effect of temperature (f) on ohmic and (g) polarisation resistance of these tests. A version of this figure has been published in a PhD thesis [47].

the absence of the Au-CCL, the ionic transport of the electrolyte is not the rate-limiting factor that dictates the ohmic behaviour of the cell. In this case, this is more likely to be determined by the electron transport between the electrode and current collector (i.e. Au-mesh). It is also evident that, whilst sintering temperatures improve the R_o values, it does not significantly alter the associated activation energy (suggesting the fundamental rate-limiting step for this process remains the same). However, the addition of the Au-CCL has an evident impact on *both* the R_o values *and* the activation energy; in these cases, the R_o activation energies appear to be dominated by the electrolyte material (indeed, the E_a values reported in Table 1 are similar to those reported for YSZ in reference [50] within a similar temperature range). Indeed, a comparison between the LSCF and LNO214 tests conducted with Au-CCL suggests very similar values (suggesting the effect of the cathode material is reduced). In the case of the R_{pol} values, the average E_a values were between 0.587 eV and 0.836 eV for LNO214 without the Au-CCL and between 1.129 eV and 1.184 eV with the Au-CCL. A comparison of literature data suggests that the data reported in this study is within the range reported by other authors (from as low as 0.44 eV [40] to as high as 1.64 eV [51]). Once more, the addition of the Au-CCL has a sizeable impact on the E_a values of the polarisation resistance (increasing to 1.184 eV from 0.710 eV), again suggesting a change in the rate-limiting process.

The aforementioned observations are of some significance in several regards. Firstly, it appears to support statements elsewhere [48,49] that link the relatively poor $La_2NiO_{4+\delta}$ performance with the inferior

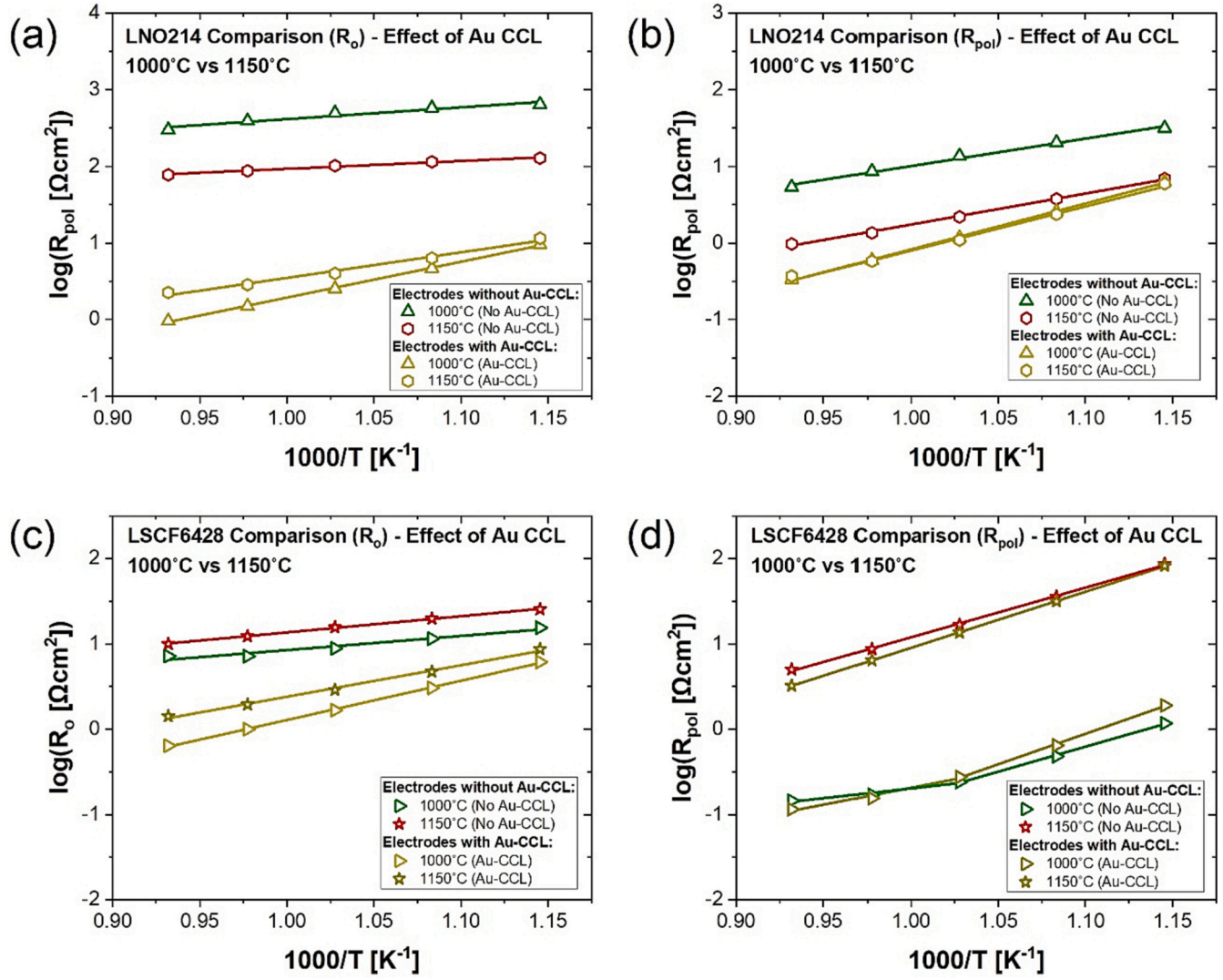

Fig. 4. Summary on the effect of the Au-CCL on the (a, c) ohmic and (b, d) polarisation values for (a, b) $La_2NiO_{4+\delta}$ and (c, d) $La_{0.6}Sr_{0.4}Co_{0.2}Fe_{0.8}O_{3-\delta}$ electrodes sintered at 1000 °C and 1150 °C. A version of this figure has been published in a PhD thesis [47].

Table 1
Activation Energy (E_a) values for symmetrical cell tests.*As is shown in the Arrhenius plots, the LSCF symmetrical cell tests were found to show two different activation energy 'regions' – in those cases, the values at lower temperature (600–700 °C) have been shown.

	Activation Energy, E_a (eV)	
Sample	R_o	R_{pol}
LNO214-1000	0.305	0.710
LNO214-1050	0.255	0.836
LNO214-1100	0.191	0.587
LNO214-1150	0.204	0.802
LNO214-1000-Au	0.928	1.184
LNO214-1150-Au	0.661	1.129
LSCF-1000*	0.329	1.161*
LSCF-1050*	0.375	1.129*
LSCF-1100	0.364	1.079
LSCF-1150	0.377	1.155
LSCF6428-1000-Au*	0.913	1.417
LSCF6428-1150-Au	0.733	1.304

electronic-conducting properties of the phase relative to LSCF6428 (and other state-of-the-art materials). The observation that R_{pol} (and not just R_o) values of $La_2NiO_{4+\delta}$ are improved via an improvement in electronic transport properties (whilst this is not the case with LSCF6428), is supportive of this conclusion. It is likely that the weak influence of the Au-CCL on the R_{pol} values of LSCF6428 is due to the already-appreciable[4] electronic conductivity of this phase (i.e. electron transport does not hugely inhibit the polarisation performance, in that instance). Secondly, the evidence here suggests that improving the electronic transport of $La_2NiO_{4+\delta}$-electrodes can considerably help in promoting electrode performance. As shown so far in this study, this can be achieved via a tailoring of sintering conditions and/or the addition of a conductive phase to act as a CCL. This offers insight into possible optimised electrode architectures (i.e. layered structures with one optimised for oxygen exchange, and a second optimised for electronic conductivity). One final point to emphasise is that the relative performance of the two materials tested here are disproportionately affected by the presence of a conductive contact paste. It is notable within the literature that many authors take many different approaches to contact configuration (e.g. different materials like Au [21] or Pt [49], use of mesh/gauze [21] or paste [49]) This will influence different materials in different ways

[4] In reference [63], LSCF6428 is shown to offer an electronic conductivity of approximately 250 to 350 S/cm under SOFC operating temperatures (i.e. 600 to 800 °C). In comparison, the conductivity of LNO214 is generally found to be lower than 100 S/cm (e.g. [11,64]).

and is probably a key cause of conflicting conclusions when comparing materials between studies.

During the symmetrical cell tests, a further side observation was noted. Study of the data hinted at the emergence of a low frequency contribution (or process) that became more dominant at higher temperatures. This was most apparent for the better-performing electrodes (e.g. LSCF6428). This arc is highlighted in the inset of Fig. 3c. The effect of this contribution is also seen in the Arrhenius plot of the R_{pol} measurements (Fig. 3f) where a divergence from the typical linear-type behaviour is seen in the case of the LSCF6428 electrode. This suggests a change in the rate-limiting process with temperature. The increasing dominance of the low frequency process at higher temperatures can be seen in supplementary Fig. S2a. Whilst this process is clear in the case of the LSCF6428 electrode, it is also observed for the $La_2NiO_{4+\delta}$ electrodes operated at higher temperatures or when employing the Au-CCL, though not as pronounced due to the overall larger R_{pol}. Importantly, the process is revealed at lower impedance values. Two further observations can be made in relation to the polarisation arc; (a) this process is not seen to be significantly affected by temperature, and (b) it is only present in the low frequency range (i.e. ~0.1 Hz). Given the described observations, it seems likely that this process is related to a gas-transport-related phenomenon. We note that a similar arc is also discussed by Primdahl and Mogensen [52].

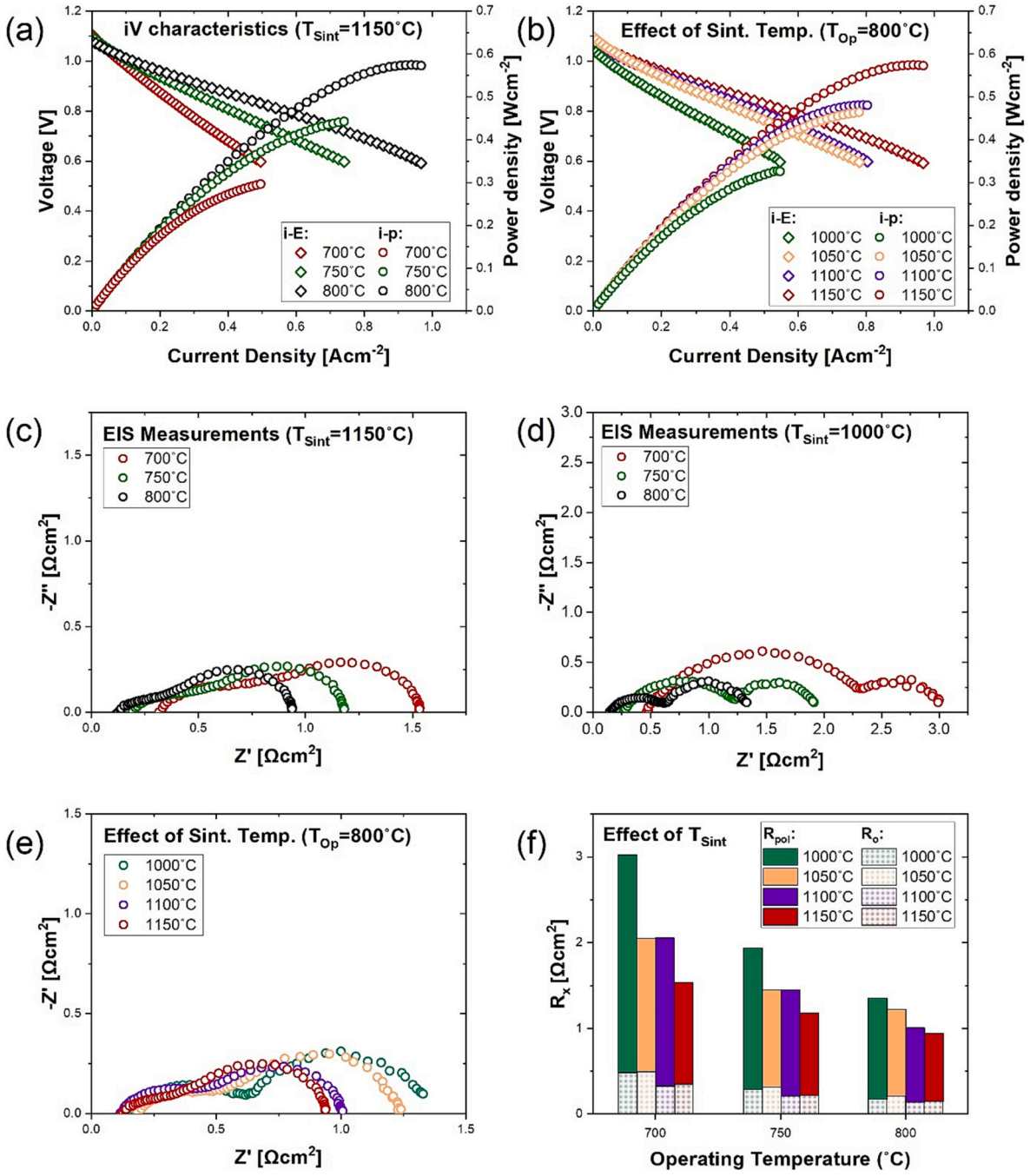

Fig. 5. Data taken from single cell tests. Current voltage characteristics of (a) $La_2NiO_{4+\delta}$ electrode sintered at 1150 °C and (b) the effect of sintering temperature on the current-voltage characteristics measured at 800 °C, (c-e) EIS measurements conducted at OCV and (f) Comparison of EIS data for electrodes sintered at 1000, 1050, 1100 and 1150 °C. A version of this figure has been published in a PhD thesis [47].

3.3. Single cell testing

A selection of the data extracted from single cell testing can be viewed in Fig. 5, with the complete set of data shown in the supplementary material (Fig. S6-S11). Broadly, the trends observed in the symmetrical cell testing are replicated; an increase in electrode sintering temperature is shown to improve the measured performance of the cell. This can be seen in relation to both the measured current output in the i-V curves (Fig. 5b) and in relation to the EIS spectra (Fig. 5e). With the former, the current density measured at 0.7 V ($i_{0.7V}$) increased from 0.42 Acm^{-2} to 0.78 Acm^{-2} at an operating temperature of 800 °C (T_{op} = 800 °C). However, despite this significant improvement, comparisons with the state-of-the-art LSCF6428 material (see supplementary Fig. S9) are not overly favourable ($i_{0.7} = 0.95 Acm^{-2}$). This appears to support observations from literature data and indicates that further measures (e.g. addition of secondary phases) are required to promote the performance of $La_2NiO_{4+\delta}$ electrodes to match that of current commercial materials.

For analysis of the EIS data taken from the single cell testing set-up, a distribution of relaxation times (DRT) analysis was employed to develop an equivalent circuit model (ECM) of the cell processes. Examples of these spectra can be viewed in the supplementary material (Supplementary Fig. S8); the spectra are comprised of 4 major peaks (or processes) which is consistent with work reported elsewhere [53]. A detailed evaluation of these processes is not presented here. The resulting model was used for an analysis of the performance-relevant parameters R_{pol} and R_o of the tested electrodes. As is highlighted by Fig. 5f, the polarisation resistance was found to decrease in those cells sintered at higher temperatures. This became increasingly apparent at the lower operating temperature of 700 °C: R_{pol} decreased from 2.53 Ωcm^2 to 1.19 Ωcm^2 by increasing the sintering temperature from 1000 to 1150 °C. These observations are consistent with the measurements conducted on symmetrical cells which were described earlier.

3.4. Ex-situ analysis

It has been shown so far that the performance of lanthanum nickelate electrodes can be significantly affected by the electrode sintering temperature. To investigate the possible causes of this observation, a series of further experiments were conducted. In the first instance, samples from the symmetrical cell tests were mounted in epoxy and polished, prior to performing SEM analysis. As can be seen in Fig. 6, an improvement in particle connectivity is achieved at the higher sintering temperatures. This offers one possible explanation for the improved performance (i.e. due to improved charge transport). This improved sintering can also be appreciated in dilatometry experiments of pressed pellets (Fig. 7). In Fig. 7a, a comparison between dilatometry experiments conducted on different materials is shown, including $La_2NiO_{4+\delta}$ and two commercial materials: $La_{0.8}Sr_{0.2}MnO_3$ and $La_{0.6}Sr_{0.4}Co_{0.2}Fe_{0.8}O_3$. The temperatures at which the pressed pellets begin to shrink is illustrated. The absolute temperature value at which this happens is perhaps less relevant than the relative differences between the samples.

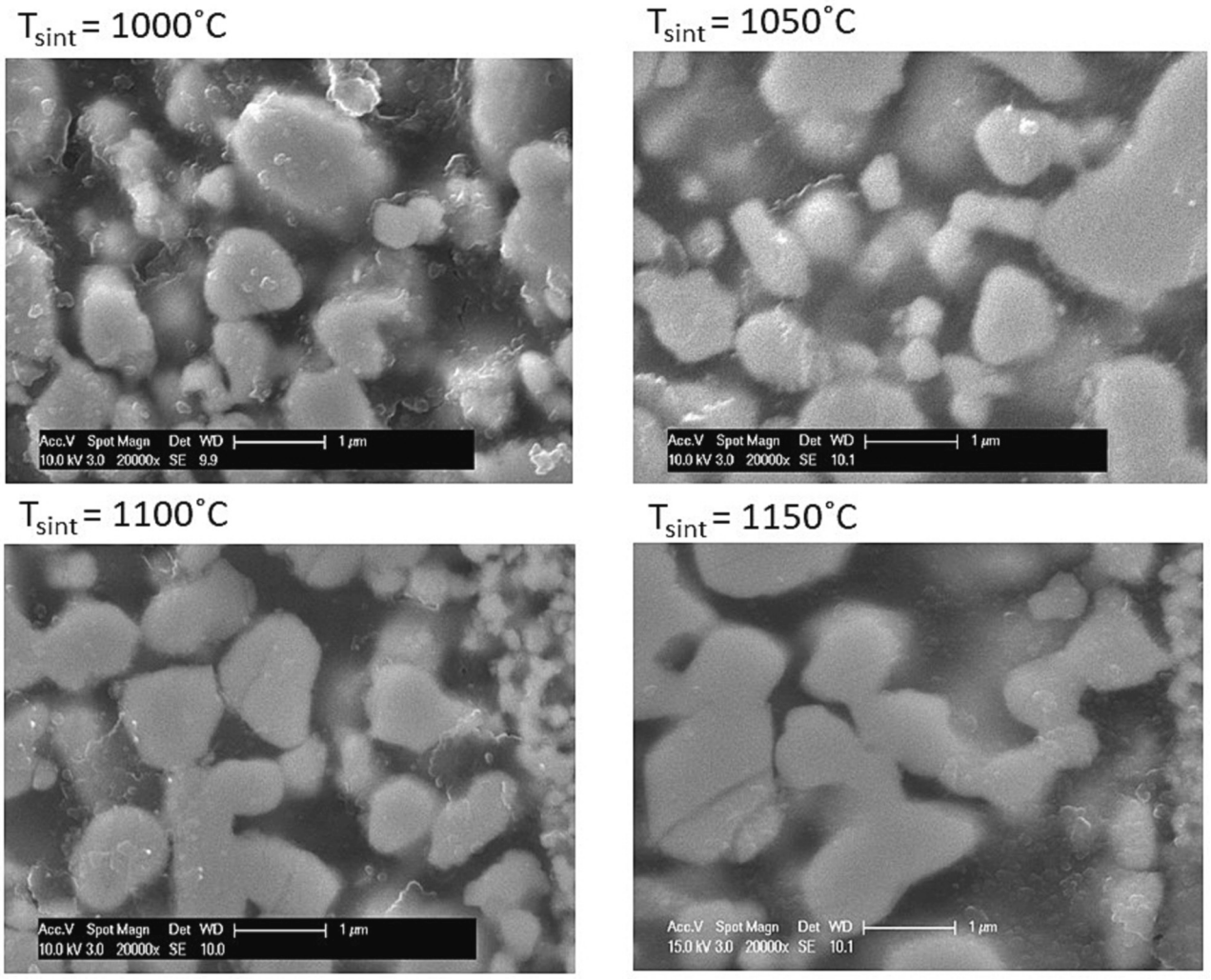

Fig. 6. Post-test SEM images of symmetrical cell tests sintered at different temperatures. *A version of this figure has been published in a PhD thesis* [47].

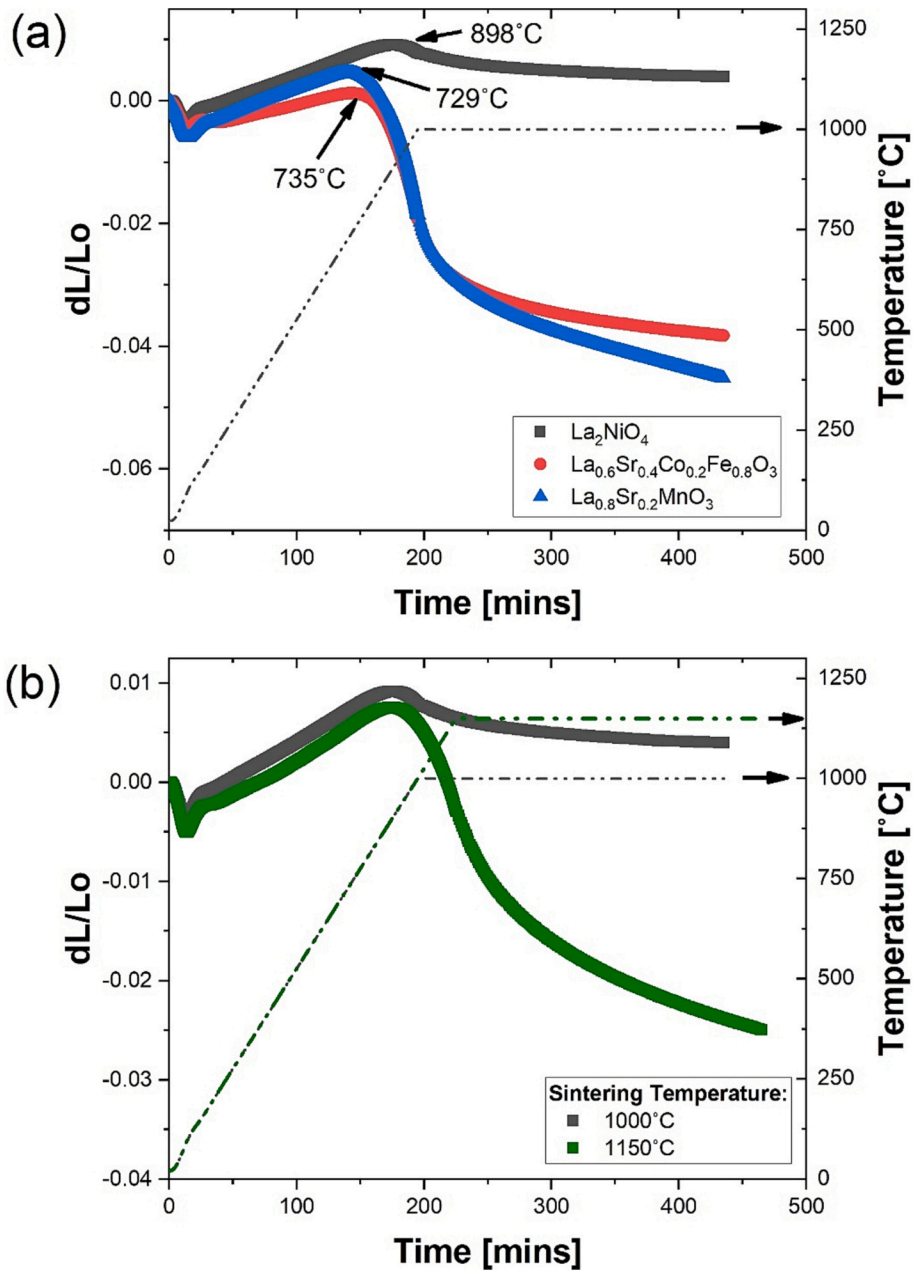

Fig. 7. Dilatometry results of (a) different phases/green pellets heated to 1000 °C and (b) a comparison of the same $La_2NiO_{4+\delta}$ heated to 1000 °C with a pellet heated to 1150 °C (employing the same temperature ramp rate and hold time). Green (un-sintered) pellets were used for this analysis to consider the relative sintering behaviours of the materials. A version of this figure has been published in a PhD thesis [47]. (For interpretation of the references to colour in this figure legend, the reader is referred to the web version of this article.)

It is evident that the lanthanum nickelate material suffers from inferior sintering characteristics relative to the Sr-containing state-of-the-art materials (that are often successfully sintered at 1000 °C) and, therefore, $La_2NiO_{4+\delta}$ can be anticipated to require higher sintering temperatures to achieve a suitable particle-connectivity. The effect of increasing the sintering temperature is shown in Fig. 7b. As would be anticipated, the volume contraction becomes more pronounced at the higher sintering temperature. Clearly, a porous electrode is favourable in the case of this application and so a completely dense body is not desirable. Therefore, a trade-off between porosity and particle coalescence is required. The evidence presented thus far suggests that the higher sintering temperatures used in this study help to achieve a more desirable electrode structure due to the improved particle adhesion.

Whilst improved particle connectivity and adhesion is likely to be achieved at higher sintering temperatures, some interactions between La-Ni-O phases and CeO_2-based materials have been previously reported [39,54]. This is suggested to be a barrier to the employment of $La_2NiO_{4+\delta}$ electrodes on CeO_2-based electrolytes or barrier layers. Indeed, some authors [22,33] have explored the use of more complex electrolyte phases to avoid this effect. Fig. 8 shows the results of powder reactivity tests between $La_2NiO_{4+\delta}$ and $Gd_{0.1}Ce_{0.9}O_2$ (GDC-10) when heated under the sintering conditions used in this study; separate mixtures of these powders were heated at 1000 and 1150 °C for 4 h. The results reveal the phases that can be expected to form at the cathode-electrolyte interface. The data indicate that lanthanum diffuses from the La-Ni-O phase into the CeO_2 phase to form a (La, Ce)O_2-type phase. The resulting La-depletion in the Ruddlesden-Popper phases leads to the formation of $La_3Ni_2O_{7-\delta}$. For comparison, the same experiment was

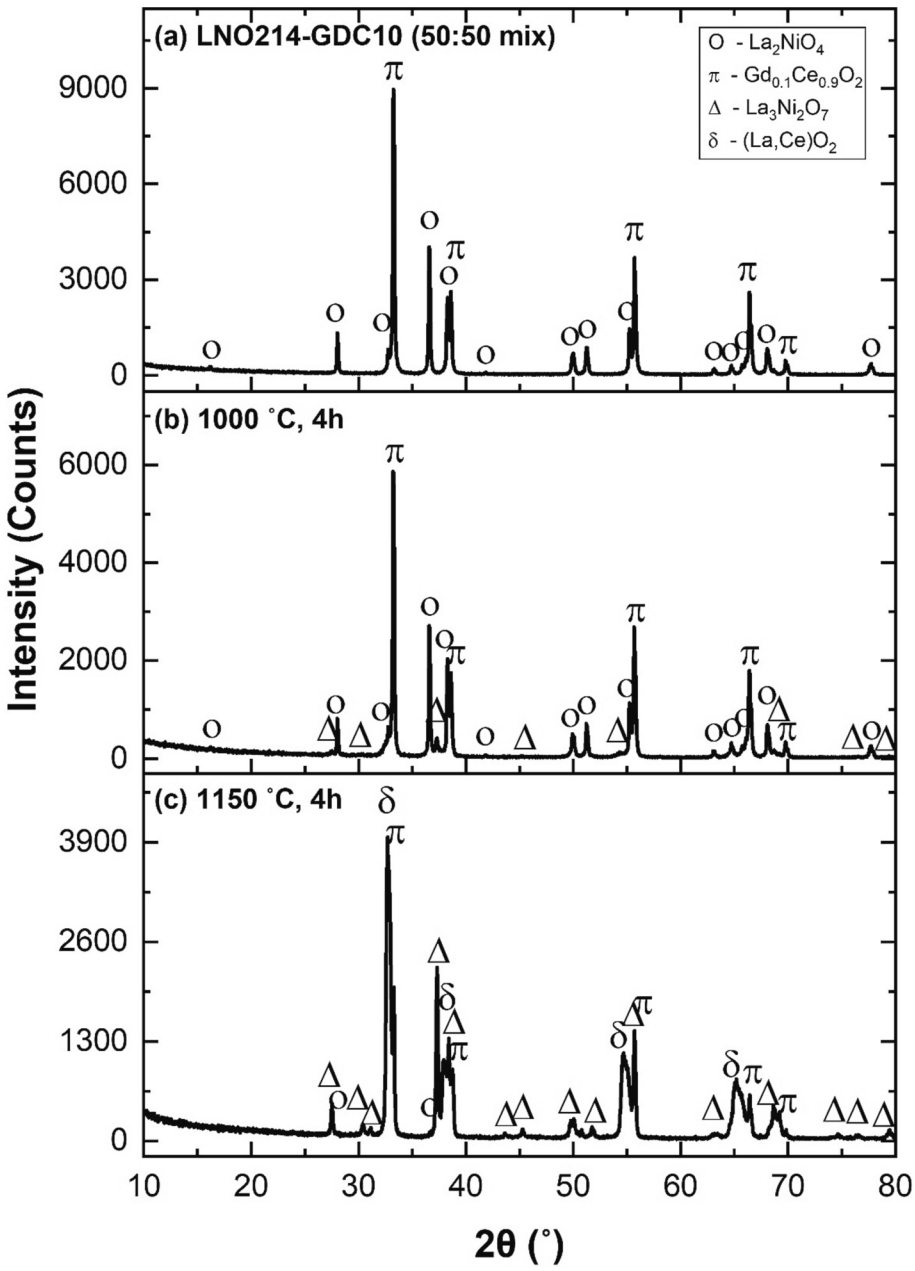

Fig. 8. XRD analysis of; (a) a mix of $La_2NiO_{4+\delta}$ (LNO214) and $Gd_{0.1}Ce_{0.9}O_2$ (GDC-10) prior to heating, (b) after heating for 4 h at 1000 °C, and (c) after heating at 1150 °C, highlighting the impurity phases seen at high temp sintering. A version of this figure has been published in a PhD thesis [47].

conducted on LSCF6428-GDC-10 powder mixes; the two materials are shown to be stable under these sintering temperatures (see supplementary Fig. S12). It is worth mentioning that the formation of $La_3Ni_2O_{7-\delta}$ may not necessarily lead to a loss in performance as, for instance, the formation of insulating phases like $La_2Zr_2O_7$ between LSCF and YSZ materials. Firstly, $La_3Ni_2O_{7-\delta}$ has been shown to offer superior electronic properties relative to $La_2NiO_{4+\delta}$ [11]. Further, a number of researchers have attempted to use La-doped Ceria as a pairing electrolyte phase and suggested favourable performances can be achieved [55,56]. The noted reaction is likely to be limited to the contact area between the two materials and so is likely to be in a very concentrated zone. The evidence from the cell testing work suggests that any such reaction does not outweigh the advantages that are obtained from higher sintering temperatures. Indeed, any formation of $La_3Ni_2O_{7-\delta}$ could be a cause of the improved performance that has been noted in this study. Two possibilities are considered:

- The improvement in performance driven by higher sintering temperatures is brought about by the improved electrode morphology (i.e. particle connectivity) and electrolyte adhesion – any detrimental effects caused by secondary phase formation are outweighed by this phenomenon.
- In addition to improvements brought about by morphological changes, the electrode performance benefits from the formation of $La_3Ni_2O_{7-\delta}$ due to better electronic conductivity relative to $La_2NiO_{4+\delta}$.

Whilst the former option seems the more plausible, the exact role of the secondary phase formation in any change in performance is difficult to categorically determine at this point.

3.5. Comparisons with literature data

As was described in the introductory section of this article, a wide body of literature data exists considering the electrode performance of single-phase $La_2NiO_{4+\delta}$ electrodes. Comparisons between data in this study and those reported by other research groups are shown in Fig. 9 and Fig. 10. Generally, the results from this study are shown to be within a similar range as the wider body of literature data. It is notable from Fig. 9 and Fig. 10 that there remain a number of other studies where better performance relative to that reported in this article has been shown to be achievable. $La_2NiO_{4+\delta}$ electrodes with improved performance have been reported relative to that observed with state-of-the-art commercial materials [20,23,26]. Whilst it is acknowledged that no significant optimisation of LSCF6428 was attempted in this study, this would appear to indicate that $La_2NiO_{4+\delta}$ can be suitably engineered to offer competitive electrode performance. However, a consideration of the better-performing $La_2NiO_{4+\delta}$ electrodes [20,23,26] in the symmetrical cell testing configuration (Fig. 9) reveals no significant cell fabrication-based trends to indicate in which way performance may be optimised. However, it is notable that in each of the referenced studies, a precious metal contact paste was employed for current collection. In two of those instances [20,23], Pt paste was utilised. The use of Pt for current collection could have contributed to the improved performance, given its good catalytic activity for the oxygen reduction reaction (ORR), in contrast to the work reported here, in which gold was used, which is known to be a poor catalyst for this process.

From the single cell testing data taken from literature (Fig. 10), the work by Lee and Kim [36] in particular is shown to offer an impressive current output with respect to single phase $La_2NiO_{4+\delta}$ electrodes. As above, in that study the authors reported the use of Pt paste and Pt mesh for current collection. Whilst it is difficult to categorically assign the cause of better performance within the literature with the use of catalytically-active metal contact pastes (such as Pt), the observations noted both in the results section of this paper and those from literature appear suggestive. From the perspective of developing $La_2NiO_{4+\delta}$ electrodes, it seems apparent that the application of conductive layers, either precious metals or other electronically-conductive ceramics such as $LaNi_{0.6}Fe_{0.4}O_3$ [9], are a necessity for this nickelate system.

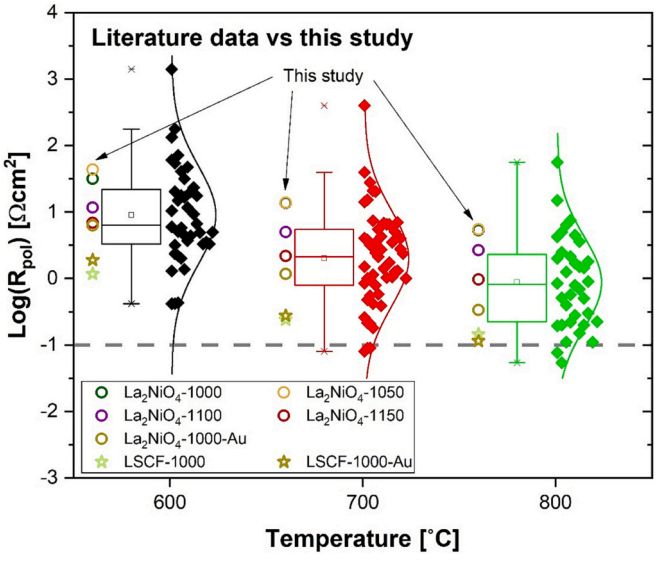

Fig. 9. Comparison between literature R_{pol} data (diamond symbols and box-whisker plot) and data from this study (La_2NiO_4 – star symbols, LSCF6428 – triangle symbols). Measurements taken at 600, 700 and 800 °C [12,15–31,40,41,51,57–59] Only results from 'single phase' electrodes are shown (i.e. composites and infiltrated electrodes are excluded). Distribution curves are shown based on the literature data. A version of this figure has been published in a PhD thesis [47].

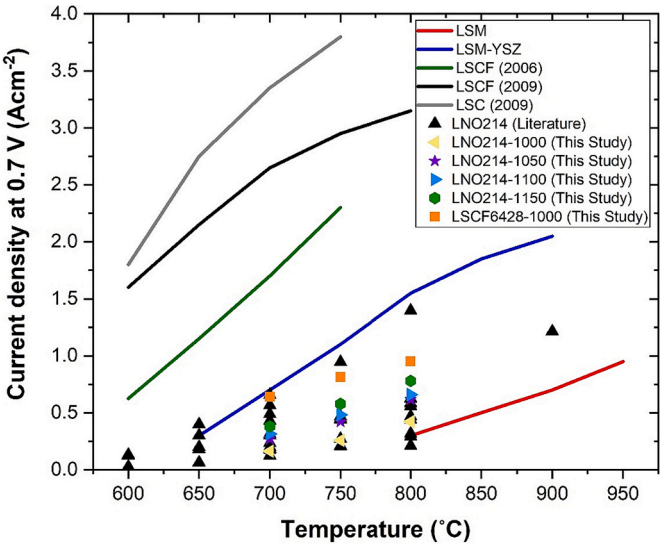

Fig. 10. Comparison between literature [2,26,32–37,60–62] $i_{0.7V}$ data and those reported in this study (also showing values measured for state-of-the-art materials at Jülich [2]). A version of this figure has been published in a PhD thesis [47].

4. Conclusions

In this study several different techniques were applied to identify the role of sintering temperatures on the performance of $La_2NiO_{4+\delta}$ electrodes in SOFC applications. A number of key points were noted:

- The performance of $La_2NiO_{4+\delta}$ was seen to improve with higher temperature sintering across both symmetrical and single cell tests – most prominently, this was shown to lead to a reduction in the ohmic resistance (R_o). Conversely, similar tests conducted on commercial LSCF6428 led to a loss in electrode performance suggesting some difference in behaviour between the two electrode materials.
- Evidence from the ex-situ tests indicated that this difference in behaviour was a result of differing sintering characteristics that, in turn, would suggest that $La_2NiO_{4+\delta}$ requires higher sintering temperatures in comparison with state-of-the-art Sr-containing materials.
- It is clear that there is a reaction between $La_2NiO_{4+\delta}$ and $Gd_{0.1}Ce_{0.9}O_2$ under typical cell fabrication conditions – this becomes increasingly evident at higher sintering temperatures. However, any detrimental effect this has on the electrode properties has not been seen to lead to considerable loss in performance in the short-term. To understand whether the instability leads to accelerated degradation rates, further long term testing is required and is identified as a topic for future work.
- Generally, the performance of $La_2NiO_{4+\delta}$ electrodes is inferior to that of LSCF6428 but significant performance improvements can be achieved by optimisation of fabrication conditions. Nevertheless, it seems likely that this material will require further optimisation by way of use of composites, infiltration, implementation of nanostructures, etc., to achieve comparable performance. This should be considered by researchers if seeking to adopt this material on the grounds of its chromium tolerance.
- The use of precious metal contact pastes in symmetrical cell tests had a profound effect on the performance of the respective electrode. This effect was shown to have variable impact dependent on the electrode material in question and its underlying properties, i.e. those with poor electronic conductivity particularly showed

improved behaviour. This should be considered when drawing comparisons across studies where different approaches to contact resistance have been applied.

Funding

This work was supported by the EPSRC via the Centre for Doctoral Training on Fuel Cells and their Fuels, grant reference EP/L015749/1, and the JUICED Hub Grant, ref. EP/R023662/1. Additionally, Dr. Sarruf acknowledges the funding received from the European Union's Horizon 2020 research and innovation programme under the Marie Skłodowska-Curie grant agreement No 101032423.

Declaration of Competing Interest

The authors declare that they have no known competing financial interests or personal relationships that could have appeared to influence the work reported in this paper.

Data availability

Data is attached as an e-component (also open to further requests for data)

Appendix A. Supplementary data

Supplementary data to this article can be found online at https://doi.org/10.1016/j.ssi.2023.116386.

References

[1] L.G.J. De Haart, J. Mougin, O. Posdziech, J. Kiviaho, N.H. Menzler, Stack degradation in dependence of operation parameters; the real-SOFC sensitivity analysis, Fuel Cells 9 (2009) 794–804, https://doi.org/10.1002/fuce.200800146.
[2] L. Blum, L.G.J. De Haart, J. Malzbender, N.H. Menzler, J. Remmel, R. Steinberger-Wilckens, Recent results in Jülich solid oxide fuel cell technology development, J. Power Sources 241 (2013) 477–485, https://doi.org/10.1016/j.jpowsour.2013.04.110.
[3] C.M. Harrison, P.R. Slater, R. Steinberger-Wilckens, A review of solid oxide fuel cell cathode materials with respect to their resistance to the effects of chromium poisoning, Solid State Ionics 354 (2020), 115410, https://doi.org/10.1016/j.ssi.2020.115410.
[4] K. Chen, S.P. Jiang, Surface segregation in solid oxide cell oxygen electrodes : phenomena, mitigation strategies and electrochemical properties, Electrochem. Energy Rev. 3 (2020) 730–765, https://doi.org/10.1007/s41918-020-00078-z.
[5] B. Koo, K. Kim, J.K. Kim, H. Kwon, J.W. Han, Sr segregation in perovskite oxides : why it happens and how it exists, Joule. 2 (2018) 1476–1499, https://doi.org/10.1016/j.joule.2018.07.016.
[6] Y. Li, W. Zhang, Y. Zheng, J. Chen, B. Yu, Y. Chen, M. Liu, Controlling cation segregation in perovskite-based electrodes for high electro-catalytic activity and durability, Chem. Soc. Rev. 46 (2017) 6345–6378, https://doi.org/10.1039/C7CS00120G.
[7] The Faraday Institution, Building a Responsible Cobalt Supply Chain, The Faraday Institution, Didcot, 2020. https://faraday.ac.uk/wp-content/uploads/2020/05/Insight-cobalt-supply-chain1.pdf.
[8] A. Petric, P. Huang, F. Tietz, Evaluation of La–Sr–Co–Fe–O perovskites for solid oxide fuel cells and gas separation membranes, Solid State Ionics 135 (2000) 719–725, https://doi.org/10.1016/S0167-2738(00)00394-5.
[9] C.M. Harrison, P.R. Slater, R. Steinberger-Wilckens, Lanthanum nickelates and their application in Solid Oxide Cells – the LaNi1-xFexO3 system and other ABO3-type nickelates, Solid State Ionics 373 (2021), 115799, https://doi.org/10.1016/j.ssi.2021.115799.
[10] M.A. Yatoo, S.J. Skinner, Ruddlesden-popper phase materials for solid oxide fuel cell cathodes: a short review, Materials Today: Proc. (2022) 10–17, https://doi.org/10.1016/j.matpr.2021.12.537.
[11] J. Song, D. Ning, B. Boukamp, J.-M. Bassat, H.J.M. Bouwmeester, Structure, electrical conductivity and oxygen transport properties of Ruddlesden–Popper phases Ln n+1 Ni n O 3n+1 (Ln = La, Pr and Nd; n = 1, 2 and 3), J. Mater. Chem. A 00 (2020) 1–16, https://doi.org/10.1039/D0TA06731H.
[12] D. Pérez-Coll, A. Aguadero, M.J. Escudero, P. Núñez, L. Daza, Optimization of the interface polarization of the La2NiO4-based cathode working with the Ce1-xSmxO2-δ electrolyte system, J. Power Sources 178 (2008) 151–162, https://doi.org/10.1016/j.jpowsour.2007.12.030.
[13] N. Schrödl, E. Bucher, A. Egger, P. Kreiml, C. Teichert, T. Höschen, W. Sitte, Long-term stability of the IT-SOFC cathode materials La0.6Sr0.4CoO3 - δ and La2NiO4 +δ against combined chromium and silicon poisoning, Solid State Ionics 276 (2015) 62–71, https://doi.org/10.1016/j.ssi.2015.03.035.
[14] S.-N. Lee, A. Atkinson, J.A. Kilner, Chromium poisoning of La2NiO4+δ cathodes, ECS Trans. 57 (2013) 605–613, https://doi.org/10.1149/05701.0605ecst.
[15] A. Aguadero, J.A. Alonso, M.J. Escudero, L. Daza, Evaluation of the La 2 Ni 1 − x Cu x O 4 + δ system as SOFC cathode material with 8YSZ and LSGM as electrolytes, Solid State Ionics 179 (2008) 393–400, https://doi.org/10.1016/j.ssi.2008.01.099.
[16] B. Philippeau, F. Mauvy, C. Mazataud, S. Fourcade, J.-C. Grenier, Comparative study of electrochemical properties of mixed conducting Ln2NiO4+δ (Ln=La, Pr and Nd) and La0.6Sr0.4Fe0.8Co0.2O3−δ as SOFC cathodes associated to Ce0.9Gd0.1O2−δ, La0.8Sr0.2Ga0.8Mg0.2O3−δ and La9Sr1Si6O26.5 electrolytes, Solid State Ionics 249–250 (2013) 17–25, https://doi.org/10.1016/j.ssi.2013.06.009.
[17] C. Solís, L. Navarrete, J.M. Serra, Study of Pr and Pr and Co doped La2NiO4+δ as cathodes for La5.5WO11.25-δ based protonic conducting fuel cells, J. Power Sources 240 (2013) 691–697, https://doi.org/10.1016/j.jpowsour.2013.05.055.
[18] R.K. Sharma, M. Burriel, L. Dessemond, V. Martin, J.M. Bassat, E. Djurado, An innovative architectural design to enhance the electrochemical performance of La2NiO4+δ cathodes for solid oxide fuel cell applications, J. Power Sources 316 (2016) 17–28, https://doi.org/10.1016/j.jpowsour.2016.03.067.
[19] R.K. Sharma, N.I. Khamidy, J. Marc Bassat, E. Djurado, La 2-X Pr x NiO 4+δ -based efficient SOFC cathodes: effect of microstructure, composition and architecture, ECS Trans. 78 (2017) 581–591, https://doi.org/10.1149/07801.0581ecst.
[20] L. Lu, Y. Guo, H. Zhang, J. Jin, Electrochemical performance of La2NiO4+δ-La0.6Sr0.4Co0.2Fe0.8O 3-δ composite cathodes for intermediate temperature solid oxide fuel cells, Mater. Res. Bull. 45 (2010) 1135–1140, https://doi.org/10.1016/j.materresbull.2010.05.031.
[21] A. Montenegro-Hernández, A. Soldati, L. Mogni, H. Troiani, A. Schreiber, F. Soldera, A. Caneiro, Reactivity at the Ln2NiO4+δ/electrolyte interface (ln = La, Nd) studied by electrochemical impedance spectroscopy and transmission Electron microscopy, J. Power Sources 265 (2014) 6–13, https://doi.org/10.1016/j.jpowsour.2014.04.082.
[22] G. Amow, I. Davidson, S. Skinner, A comparative study of the Ruddlesden-Popper series, Lan+1NinO3n+1 (n=1, 2 and 3), for solid-oxide fuel-cell cathode applications, Solid State Ionics 177 (2006) 1205–1210, https://doi.org/10.1016/j.ssi.2006.05.005.
[23] M. Rieu, R. Sayers, M.A. Laguna-Bercero, S.J. Skinner, P. Lenormand, F. Ansart, Investigation of graded La2NiO4+δ cathodes to improve SOFC electrochemical performance, J. Electrochem. Soc. 157 (2010) B477–B480, https://doi.org/10.1149/1.3298439.
[24] V. Vibhu, A. Rougier, J.-C. Grenier, J.-M. Bassat, Mixed nickelates Pr2-XLaxNiO4+ used as cathodes in metal supported SOFCs, ECS Trans. 57 (2013) 2093–2100, https://doi.org/10.1149/05701.2093ecst.
[25] T.W. Chiu, Y.T. Lin, I.F. Yen, H.H. Hsieh, S.F. Wang, Properties and performance of La2NiO4+δ- LaNiO3 composite cathodes for intermediate-temperature solid oxide fuel cells, Ferroelectrics. 457 (2013) 105–110, https://doi.org/10.1080/00150193.2013.848763.
[26] X. Zhang, L. Zhang, J. Meng, W. Zhang, F. Meng, X. Liu, J. Meng, Highly enhanced electrochemical property by mg-doping La2Ni1-xMgxO4+Δ (x = 0.0, 0.02, 0.05 and 0.10) cathodes for intermediate-temperature solid oxide fuel cells, Int. J. Hydrog. Energy 42 (2017) 29498–29510, https://doi.org/10.1016/j.ijhydene.2017.10.091.
[27] M.J. Escudero, A. Aguadero, J.A. Alonso, L. Daza, A kinetic study of oxygen reduction reaction on La2NiO4 cathodes by means of impedance spectroscopy, J. Electroanal. Chem. 611 (2007) 107–116, https://doi.org/10.1016/j.jelechem.2007.08.006.
[28] F. Chauveau, J. Mougin, F. Mauvy, J.-M. Bassat, J.C. Grenier, Electrochemical performances of cells containing alternative oxygen electrodes, ln 2 NiO 4+δ (ln=Nd, La), ECS Trans. 25 (2009) 2557–2564, https://doi.org/10.1149/1.3205812.
[29] R. Sayers, M. Rieu, P. Lenormand, F. Ansart, J.A. Kilner, S.J. Skinner, Development of lanthanum nickelate as a cathode for use in intermediate temperature solid oxide fuel cells, Solid State Ionics 192 (2011) 531–534, https://doi.org/10.1016/j.ssi.2010.02.014.
[30] K. Zhao, Q. Xu, D.P. Huang, W. Chen, M. Chen, B.H. Kim, Microstructure and electrochemical properties of porous La 2NiO 4+δ electrode screen-printed on Ce 0.8Sm 0.2O 1.9 electrolyte, J. Solid State Electrochem. 16 (2012) 9–16, https://doi.org/10.1007/s10008-010-1270-y.
[31] M. Ferkhi, A. Ringuedé, A. Khaled, L. Zerroual, M. Cassir, La 1.98Ni0 4±δ, a new cathode material for solid oxide fuel cell: impedance spectroscopy study and compatibility with gadolinia-doped ceria and yttria-stabilized zirconia electrolytes, Electrochim. Acta 75 (2012) 80–87, https://doi.org/10.1016/j.electacta.2012.04.064.
[32] H. Tang, Z. Jin, Y. Wu, W. Liu, L. Bi, Cobalt-free nanofiber cathodes for proton conducting solid oxide fuel cells, Electrochem. Commun. 100 (2019) 108–112, https://doi.org/10.1016/j.elecom.2019.01.022.
[33] M.J. Escudero, A. Fuerte, L. Daza, La2NiO4+δ potential cathode material on La 0.9Sr0.1Ga0.8Mg0.2O2.85 electrolyte for intermediate temperature solid oxide fuel cell, J. Power Sources 196 (2011) 7245–7250, https://doi.org/10.1016/j.jpowsour.2010.11.068.
[34] G. Yang, C. Su, R. Ran, M.O. Tade, Z. Shao, Advanced symmetric solid oxide fuel cell with an infiltrated K 2NiF4-type La2NiO4 electrode, Energy Fuel 28 (2014) 356–362, https://doi.org/10.1021/ef401473w.
[35] A.N. Koval'chuk, A.V. Kuz'min, D.A. Osinkin, A.S. Farlenkov, A.A. Solov'ev, A. V. Shipilova, I.V. Ionov, N.M. Bogdanovich, S.M. Beresnev, Single SOFC with supporting Ni-YSZ anode, bilayer YSZ/GDC film electrolyte, and La2NiO4 + δ cathode, Russ. J. Electrochem. 54 (2018) 541–546, https://doi.org/10.1134/S1023193518060101.

[36] Y. Lee, H. Kim, Electrochemical performance of La2NiO4+δ cathode for intermediate-temperature solid oxide fuel cells, Ceram. Int. 41 (2015) 5984–5991, https://doi.org/10.1016/j.ceramint.2015.01.037.
[37] K. Zhao, Y.P. Wang, M. Chen, Q. Xu, B.H. Kim, D.P. Huang, Electrochemical evaluation of La2NiO4+δ as a cathode material for intermediate temperature solid oxide fuel cells, Int. J. Hydrog. Energy 39 (2014) 7120–7130, https://doi.org/10.1016/j.ijhydene.2014.02.106.
[38] R. Sayers, J.E. Parker, C.C. Tang, S.J. Skinner, In situ compatibility studies of lanthanum nickelate with a ceria-based electrolyte for SOFC composite cathodes, J. Mater. Chem. 22 (2012) 3536–3543, https://doi.org/10.1039/c2jm14384d.
[39] R. Sayers, J. Liu, B. Rustumji, S.J. Skinner, Novel K 2 NiF 4 -type materials for solid oxide fuel cells: compatibility with electrolytes in the intermediate temperature range, Fuel Cells 8 (2008) 338–343, https://doi.org/10.1002/fuce.200800023.
[40] X. Ye, H. Luo, M. Hou, P. Bertrand, A. Billard, P. Briois, Morphological evolution of La2NiO4 coatings synthesized by reactive magnetron sputtering (RMS) at high pressure as cathode for intermediate temperature solid oxide fuel cell (IT-SOFC), Coatings. 13 (2023) 1113, https://doi.org/10.3390/coatings13061113.
[41] K.A. Kuterbekov, K.Z. Bekmyrza, A.M. Kabyshev, M.M. Kubenova, N. K. Aidarbekov, S.A. Nurkenov, Investigation of the characteristics of materials with the Ruddlesden-popper structure for solid oxide fuel cells, Bulletin of the Karaganda University. "Physics" Series. 108 (2022) 32–47, https://doi.org/10.31489/2022ph4/32-47.
[42] E. Niwa, C. Uematsu, T. Hashimoto, Sintering temperature dependence of conductivity, porosity and specific surface area of LaNi0.6Fe0.4O3 ceramics as cathode material for solid oxide fuel cells - superiority of Pechini method among various solution mixing processes, Mater. Res. Bull. 48 (2013) 1–6, https://doi.org/10.1016/j.materresbull.2012.09.055.
[43] G. Amow, I.J. Davidson, Preliminary investigation of the higher-order ruddlesden-popper phases for IT-SOFC cathodes, Lan+1NinO3n+1 (n = 2 and 3), Proceedings - Electrochemical Society. PV 2005-07, 2005, pp. 1745–1750, https://doi.org/10.1149/200507.1745pv.
[44] A.E. Danks, S.R. Hall, Z. Schnepp, The evolution of "sol-gel" chemistry as a technique for materials synthesis, Mater. Horiz. 3 (2016) 91–112, https://doi.org/10.1039/c5mh00260e.
[45] D. Klotz, A. Weber, E. Ivers-Tiffée, Practical guidelines for reliable electrochemical characterization of solid oxide fuel cells, Electrochim. Acta 227 (2017) 110–126, https://doi.org/10.1016/j.electacta.2016.12.148.
[46] A. Mehta, P.J. Heaney, Structure of La2NiO4.18, Phys. Rev. B 49 (1994) 563–571, https://doi.org/10.1103/PhysRevB.49.563.
[47] C.M. Harrison, A Study Lanthanum Nickelate Cathodes for Employment in Solid Oxide Fuel Cells, University of Birmingham, 2023.
[48] H. Tang, Z. Gong, Y. Wu, Z. Jin, W. Liu, Electrochemical performance of nanostructured LNF infiltrated onto LNO cathode for BaZr0.1Ce0.7Y0.2O3-d-based solid oxide fuel cell, Int. J. Hydrog. Energy 43 (2018) 19749–19756, https://doi.org/10.1016/j.ijhydene.2018.09.008.
[49] M. Chen, B.H. Moon, S.H. Kim, B.H. Kim, Q. Xu, B.-G. Ahn, Characterization of La0.6Sr0.4Co0.2Fe0.8O3-δ + La2NiO4+δ composite cathode materials for solid oxide fuel cells, Fuel Cells 12 (2012) 86–96, https://doi.org/10.1002/fuce.201100106.
[50] C. Ahamer, A.K. Opitz, G.M. Rupp, J. Fleig, Revisiting the temperature dependent ionic conductivity of Yttria Stabilized Zirconia (YSZ), J. Electrochem. Soc. 164 (2017) F790–F803, https://doi.org/10.1149/2.0641707jes.
[51] A.R. Gilev, E.A. Kiselev, K.S. Sukhanov, D.V. Korona, V.A. Cherepanov, Evaluation of La2-x(Ca/Sr)xNi1-yFeyO4+d (x=0.5, 0.6; y=0.4, 0.5) as cathodes for proton-conducting SOFC based on lanthanum tungstate, Electrochim. Acta 421 (2022) 140479, https://doi.org/10.1016/j.electacta.2022.140479.
[52] S. Primdahl, M. Mogensen, Gas conversion impedance: a test geometry effect in characterization of solid oxide fuel cell anodes, J. Electrochem. Soc. 145 (1998) 2431–2438, https://doi.org/10.1149/1.1838654.
[53] A. Leonide, V. Sonn, A. Weber, E. Ivers-Tiffée, Evaluation and modeling of the cell resistance in anode-supported solid oxide fuel cells, J. Electrochem. Soc. 155 (2008) B36–B41, https://doi.org/10.1149/1.2801372.
[54] A.M. Hernández, L. Mogni, A. Caneiro, La2NiO4+δ as cathode for SOFC: reactivity study with YSZ and CGO electrolytes, Int. J. Hydrog. Energy 35 (2010) 6031–6036, https://doi.org/10.1016/j.ijhydene.2009.12.077.
[55] P. Li, X. Huang, B. Wei, Z. Wang, Y. Zhang, X. Zhu, L. Zhang, L. Zhu, Z. Lü, A novel La2NiO4+d-La3Ni2O7-d-Ce0.55La0.45O2-d ternary composite cathode prepared by the co-synthesis method for IT-SOFCs, Int. J. Hydrog. Energy 42 (2017) 17202–17210, https://doi.org/10.1016/j.ijhydene.2017.05.202.
[56] Y. Shen, H. Zhao, J. Xu, X. Zhang, K. Zheng, K. Świerczek, Effect of ionic size of dopants on the lattice structure, electrical and electrochemical properties of La2-xMxNiO 4+δ (M = Ba, Sr) cathode materials, Int. J. Hydrog. Energy 39 (2014) 1023–1029, https://doi.org/10.1016/j.ijhydene.2013.10.153.
[57] J. Fondard, A. Billard, G. Bertrand, P. Briois, Ln2NiO4+δ (Ln = La, Pr, Nd) coatings deposited by reactive magnetron sputtering as cathode material for intermediate temperature solid oxide fuel cell, Vacuum. 152 (2018) 97–108, https://doi.org/10.1016/j.vacuum.2018.03.013.
[58] C. Yao, J. Yang, H. Zhang, S. Chen, J. Meng, K. Cai, Evaluation of bismuth doped La2-xBixNiO4+δ (x = 0, 0.02 and 0.04) as cathode materials for solid oxide fuel cells, Ceram. Int. 47 (2021) 24589–24596, https://doi.org/10.1016/j.ceramint.2021.05.179.
[59] L. Navarrete, M. Fabuel, C.Y. Yoo, J.M. Serra, Tailoring La2-XAXNi1-YBYO4+δ cathode performance by simultaneous A and B doping for IT-SOFC, Int. J. Hydrog. Energy 45 (2020) 15589–15599, https://doi.org/10.1016/j.ijhydene.2020.03.150.
[60] Y. Gong, R. Wang, J. Banner, S.N. Basu, U.B. Pal, S. Gopalan, Improved tolerance of lanthanum nickelate (La2NiO4+δ) cathodes to chromium poisoning under current load in solid oxide fuel cells, Jom. 71 (2019) 3848–3858, https://doi.org/10.1007/s11837-019-03724-0.
[61] C.Y. Gu, X.S. Wu, J.F. Cao, J. Hou, L.N. Miao, Y.P. Xia, W. Liu Chao-Fu, High performance Ca-containing La2-xCaxNiO4+δ(0≤x≤0.75) cathode for proton-conducting solid oxide fuel cells, Int. J. Hydrog. Energy 45 (2020) 23422–23432, https://doi.org/10.1016/j.ijhydene.2020.06.106.
[62] X. Li, D. Huan, N. Shi, Y. Yang, Y. Wan, C. Xia, R. Peng, Y. Lu, Defects evolution of Ca doped La2NiO4+δ and its impact on cathode performance in proton-conducting solid oxide fuel cells, Int. J. Hydrog. Energy 45 (2020) 17736–17744, https://doi.org/10.1016/j.ijhydene.2020.04.150.
[63] L.-W. Tai, M.M. Nasrallah, H.U. Anderson, D.M. Sparlin, S.R. Sehlin, Structure and electrical properties of La1 − xSrxCo1 − yFeyO3. Part 2. The system La1 − xSrxCo0.2Fe0.8O3, Solid State Ionics 76 (1995) 273–283, https://doi.org/10.1016/0167-2738(94)00245-N.
[64] D.O. Bannikov, V.A. Cherepanov, Thermodynamic properties of complex oxides in the La–Ni–O system, J. Solid State Chem. 179 (2006) 2721–2727, https://doi.org/10.1016/j.jssc.2006.05.026.